Analytical studies of the magnetic domain wall structure in the presence of non-uniform exchange bias

Cite as: AIP Advances **11**, 065308 (2021); https://doi.org/10.1063/5.0046803
Submitted: 09 February 2021 . Accepted: 13 May 2021 . Published Online: 03 June 2021

Yee-Mou Kao, Lance Horng, and Chi-Ho Cheng

Analytical studies of the magnetic domain wall structure in the presence of non-uniform exchange bias

Cite as: AIP Advances 11, 065308 (2021); doi: 10.1063/5.0046803
Submitted: 9 February 2021 • Accepted: 13 May 2021 •
Published Online: 3 June 2021

Yee-Mou Kao,[a] Lance Horng, and Chi-Ho Cheng[b]

AFFILIATIONS

Department of Physics, National Changhua University of Education, Changhua 500, Taiwan

[a]ymkao@cc.ncue.edu.tw
[b]Author to whom correspondence should be addressed: phcch@cc.ncue.edu.tw

ABSTRACT

The pinning phenomena of the domain wall in the presence of exchange bias are studied analytically. The analytic solution of the domain wall spin configuration is presented. Unlike the traditional solution, which is symmetric, our new solution could exhibit the asymmetry of the domain wall spin profile. Using the solution, the domain wall position, its width, its stability, and the depinning field are discussed analytically.

I. INTRODUCTION

Magnetic recording has been the most successful method for data storage in the last few decades. In 2008, Parkin *et al.* proposed a racetrack memory that has all the advantages of magnetoresistance random access memory (MRAM) and an all-metallic semiconductor free structure.[1] Racetrack memory consists of a ferromagnetic wire where a magnetic domain wall (DW) can be injected and detected. A 180° transverse DW carries a data bit via its configuration of either north to north or south to south poles. Several directions were proposed to apply nanofabrication techniques to geometrically control the DW width and shape.[2] Artificially induced defects could be used as pinning sites, while nanopatterned structures provide modification of the DW's configuration, size, and dynamical properties.[3]

Recently, it was found that the pinning site, e.g., notch, may generate topological defects and then change the chirality and topological properties of the DW structure. The chirality of the DW will affect its trajectory in a Y-shaped wire.[4,5] Topological defect pinning may not be a good option for data storage.

Another option is making use of the exchange bias effect to pin the DW in the ferromagnetic material, which could be more stable and smaller in size. As illustrated in Fig. 1, the DW is generated in the ferromagnetic (F) wire.[6] The pinning is controlled through the exchange bias induced by the antiferromagnetic (AF) wire. Its possibility was recently realized in experiments[7] and simulation.[8] However, its theoretical understanding is still lacking.

In extreme conditions, without the magnetostatic and surface energies, only the anisotropy and exchange energies are considered, and the spin orientation near the domain wall[9,10] reads

$$\theta(x) = 2\tan^{-1}\left[\exp\left(\frac{x}{\lambda}\right)\right], \tag{1}$$

describing a head-to-head block wall in the x-direction with a spin angle $\theta(x)$.[11] $\lambda = \sqrt{A_{ex}/K}$, with A_{ex} being the exchange stiffness and K being the anisotropy constant along the x-axis. This formula gives the domain wall width $\delta_{DW} \simeq \pi\lambda$ and the energy density $\varepsilon_{DW} = 4\sqrt{A_{ex}K}$.

For thin magnetic nanowires, since the shape anisotropy is mainly determined by the thickness and width of the nanowires, the anisotropy should be perpendicular or in-plane.[12,13] In this paper, only the in-plane case is considered for simplicity. The analytic solution of the domain wall profile is obtained. With the help of the analytic solution, the relationship between spin orientation and the length scales of the domain wall is derived. The position of the domain wall, its width, and its stability are also discussed.

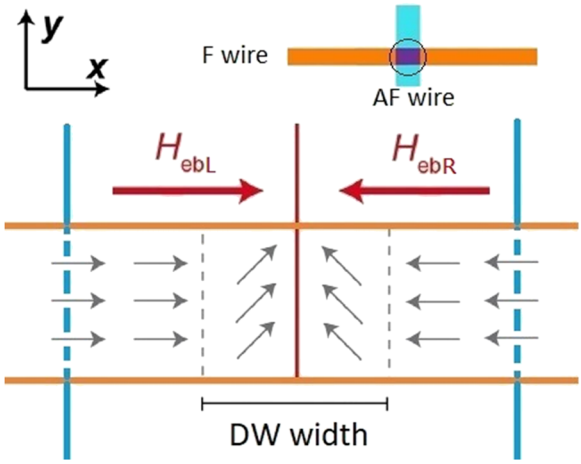

FIG. 1. Illustration of the exchange bias field (red arrows) and magnetization vectors (gray arrows) in the F wire. The AF wire boundary is marked by blue lines. The domain wall region is identified by gray dashed lines. The exchange bias fields—H_{ebL} in the left and H_{ebR} in the right—are oriented in opposite directions.

II. MODEL FOR NON-UNIFORM EXCHANGE BIAS

In ferromagnetic material, two magnetic atoms interact with the so-called exchange interaction, $J\vec{S}_1 \cdot \vec{S}_2$. J is the exchange constant, and $\vec{S}_1$ and $\vec{S}_2$ are the magnetic moments of the two atoms. In one-dimensional wire and a continuum limit, suppose the atoms only interact with their nearest neighbors and the direction of magnetization varies slowly along the wire, then the energy, which we call the exchange energy E_{ex}, is

$$E_{ex} = A_{ex}\int_{-\infty}^{+\infty} dx\left(\frac{d\theta}{dx}\right)^2 \tag{2}$$

up to a constant. A_{ex}, which is proportional to J, is called the exchange constant. $\theta(x)$ is the orientation of the magnetization at position x.

If we further consider the coupling between the ferromagnetic material and another antiferromagnet, a unidirectional anisotropy would be induced in the ferromagnetic material, which is usually referred to as exchange bias.[14] The corresponding exchange bias energy density could be modeled by

$$\varepsilon_{eb} = -K_{eb}\cos(\theta(x) - \theta_{eb}), \tag{3}$$

where K_{eb} is called the unidirectional exchange coupling constant. θ_{eb} is the angle between the magnetic moment and unidirectional anisotropy axes.

In our system, as illustrated in Fig. 1, besides the exchange energy of the F wire, there is also the exchange bias energy E_{eb} due to the coupling between the F and AF wires. At the interface between F and AF wires, the exchange anisotropy effect could create the domain wall in the F wire. As shown in Fig. 1, in the left (right) hand side of the F wire, the magnetization points to the right (left) due to the coupling from the AF wire. Hence,

$$\theta_{eb} = \begin{cases} 0 & \text{if } x < 0 \\ \pi & \text{if } x > 0, \end{cases} \tag{4}$$

and K_{eb} is also different in the left and right sides. We define the exchange bias field $\vec{H}_{eb}$ such that its magnitude $H_{eb} = K_{eb}/M_s$, where M_s is the saturation magnetization of the F wire. The direction of $\vec{H}_{eb}$ is along the unidirectional anisotropy axes. It follows that

$$\vec{H}_{eb} = \begin{cases} H_{ebL}\,\hat{e}_x & \text{if } x < 0 \\ -H_{ebR}\,\hat{e}_x & \text{if } x > 0, \end{cases} \tag{5}$$

where H_{ebL} and H_{ebR} are the exchange bias field intensities in the left and right regions, respectively. The domain wall width in the range of 150 nm to 1 μm can be obtained at the boundary between two regions with opposite exchange bias fields ranging from 50 to 300 Oe. These exchange bias values are compatible with those found in the $Fe_{40}Co_{40}B_{20}/Ir_{20}Mn_{80}$ or $Py/Ir_{20}Mn_{80}$ systems.[15]

Equation (3) can then be re-written as

$$\varepsilon_{eb} = -\vec{M} \cdot \vec{H}_{eb}, \tag{6}$$

where $\vec{M} = M_s(\hat{e}_x \cos\theta(x) + \hat{e}_y \sin\theta(x))$. It turns out that the exchange bias energy

$$E_{eb} = -\int_{-\infty}^{+\infty} dx\vec{M} \cdot \vec{H}_{eb}. \tag{7}$$

The pinning of the DW by exchange bias with two regions characterized by different unidirectional anisotropy was proposed by Albisetti and Petti.[8]

III. DOMAIN WALL STRUCTURE

Combining the exchange energy E_{ex} in Eq. (2) and the exchange bias energy E_{eb} in Eq. (7), we get the DW energy

$$E = A_{ex}\int_{-\infty}^{+\infty} dx\left(\frac{d\theta}{dx}\right)^2 - \int_{-\infty}^{+\infty} dx\vec{M} \cdot \vec{H}_{eb}. \tag{8}$$

The DW profiles are determined by competition. Decomposing the DW energy into two regions leads to

$$E = \int_0^{\infty} dx\left[A_{ex}\left(\frac{d\theta}{dx}\right)^2 + M_s H_{ebR}\cos\theta\right] + \int_{-\infty}^{0} dx\left[A_{ex}\left(\frac{d\theta}{dx}\right)^2 - M_s H_{ebL}\cos\theta\right]. \tag{9}$$

Minimization with respect to $\theta(x)$ gives

$$2A_{ex}\frac{d^2\theta}{dx^2} - M_s H_{ebL}\sin\theta = 0 \quad \text{if} \quad x < 0, \tag{10}$$

$$2A_{ex}\frac{d^2\theta}{dx^2} + M_s H_{ebR}\sin\theta = 0 \quad \text{if} \quad x > 0 \tag{11}$$

with the boundary conditions

$$\lim_{x\to-\infty}\theta(x) = 0, \tag{12}$$

$$\lim_{x\to+\infty}\theta(x) = \pi, \tag{13}$$

and furthermore, the continuity imposed at $x = 0$ gives $\theta(x = 0) = \theta_0$ as an undetermined parameter. The solution is found to be

$$\theta(x) = \begin{cases} 4\tan^{-1}\left[\tan\left(\frac{\theta_0}{4}\right)\exp\left(\frac{x}{\lambda_L}\right)\right] & \text{if} \quad x < 0 \\ \pi - 4\tan^{-1}\left[\tan\left(\frac{\pi-\theta_0}{4}\right)\exp\left(-\frac{x}{\lambda_R}\right)\right] & \text{if} \quad x > 0, \end{cases} \tag{14}$$

where $\lambda_L = \sqrt{2A_{ex}/(M_s H_{ebL})}$ and $\lambda_R = \sqrt{2A_{ex}/(M_s H_{ebR})}$ define the length scales of the domain wall in the left and right regions, respectively. Here, we obtained a formula different from the traditional one used in micromagnetics, as shown in Eq. (1). The traditional formula is applied for the head-to-head block wall whereas it is the Néel wall in our case. The spin orientation at $x = 0$, θ_0, is determined by the continuity of its derivatives, i.e., $\theta'(x = 0^-) = \theta'(x = 0^+)$, which gives

$$\theta_0 = 2\tan^{-1}\left(\frac{\lambda_L}{\lambda_R}\right). \tag{15}$$

If the bias field is symmetric, i.e., $H_{ebL} = H_{ebR}$, then $\lambda_L = \lambda_R$, $\theta_0 = \pi/2$, and obviously, the DW center $x_c = 0$ by symmetry. In general, the bias field is not necessary to be symmetric, i.e., $H_{ebL} \neq H_{ebR}$, and the DW width becomes $\delta_{DW} = \pi(\lambda_L + \lambda_R)/2$.[16] The DW center, x_c, defined as the position such that $\theta(x_c) = \pi/2$, can be found by using Eqs. (14) and (15), which is

$$x_c = \begin{cases} \lambda_R\left[\ln\left(\sqrt{2}+1\right) - \ln\left(\frac{\sqrt{\lambda_L^2+\lambda_R^2}+\lambda_L}{\lambda_R}\right)\right] & \text{if} \quad H_{ebL} > H_{ebR} \\ -\lambda_L\left[\ln\left(\sqrt{2}+1\right) - \ln\left(\frac{\sqrt{\lambda_L^2+\lambda_R^2}+\lambda_R}{\lambda_L}\right)\right] & \text{if} \quad H_{ebL} < H_{ebR}. \end{cases} \tag{16}$$

If the lowest order is kept, the expression can be simplified as

$$x_c = \frac{1}{\sqrt{2}}(\lambda_R - \lambda_L) \tag{17}$$

for $|\lambda_L - \lambda_R| \ll \lambda_L$ and $|\lambda_L - \lambda_R| \ll \lambda_R$. This serves as a useful formula for fast estimation of the domain wall center position. The spin orientation $\theta(x)$ along the F wire for different biases is shown in Fig. 2. It can be seen that as the bias field asymmetry increases, the domain wall becomes wider, and the domain wall center will shift to the direction of lower bias. It implies that one can fine-tune the DW position and modify the DW width through exchange bias. To quantify their changes, let the dimensional parameter $h = \frac{H_{ebL}-H_{ebR}}{H_{ebL}+H_{ebR}}$ to represent the degree of asymmetry bias. The DW width and the center position can then be re-written as

$$\begin{aligned} \delta_{DW} &= \frac{\pi}{2}\sqrt{\frac{A_{ex}}{M_s(H_{ebL}+H_{ebR})}}\left[(1+h)^{-1/2} + (1-h)^{-1/2}\right] \\ &= \pi\sqrt{\frac{A_{ex}}{M_s(H_{ebL}+H_{ebR})}}\left[1 + \frac{3}{8}h^2 + \frac{35}{128}h^4 + O(h^6)\right] \end{aligned} \tag{18}$$

and

$$x_c = \sqrt{\frac{A_{ex}}{2M_s(H_{ebL}+H_{ebR})}}h\left(1 + \frac{1}{4}|h| + \frac{13}{24}|h|^2 + O(|h|^3)\right). \tag{19}$$

The plots of their relationship with h are shown in Fig. 3.

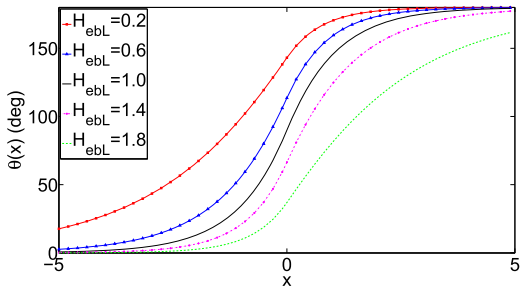

FIG. 2. Spin orientation $\theta(x)$ as a function of x in the unit of length scale $\sqrt{\frac{A_{ex}}{M_s(H_{ebL}+H_{ebR})}}$ for different H_{ebL} in the unit of $(H_{ebL} + H_{ebR})/2$.

If an external magnetic field $\vec{H}_{ext} = H_{ext}\hat{e}_x$ is applied along the F wire, the bias asymmetry is modified, so it turns out to be described by an effective exchange bias field $\vec{H}_{eb}^{eff}$, which is the sum of $\vec{H}_{eb}$ from Eq. (5) and $\vec{H}_{ext}$, i.e.,

$$\vec{H}_{eb}^{eff} = \begin{cases} (H_{ebL} + H_{ext})\,\hat{e}_x & \text{if} \quad x < 0 \\ (-H_{ebR} + H_{ext})\,\hat{e}_x & \text{if} \quad x > 0. \end{cases} \tag{20}$$

When the applied field H_{ext} approaches the exchange bias in the right region, H_{ebR}, the corresponding DW width in the right, which is described by the length scale $\sqrt{2A_{ex}/(M_s(H_{ebR} - H_{ext}))}$, will diverge. Physically, it implies that the domain wall becomes unstable. Such a critical external field,

$$H_c = H_{ebR}, \tag{21}$$

should correspond to the depinning field with the same order of magnitude. It is consistent with the experimental observation that the wider the AF wires, the larger the exchange bias, and hence, the larger the depinning field.[7]

The variation in E_{eb} is justified in polycrystalline exchange bias systems characterized by large antiferromagnetic uniaxial anisotropy.[17] In $Fe_{40}Co_{40}B_{20}/Ir_{20}Mn_{80}$ systems, the typical values of saturation magnetization $M_s = 750$ kA/m, exchange stiffness $A_{ex} = 1.2 \times 10^{-11}$ J/m, and if H_{eb} is 175 Oe, then $\lambda_H \simeq 42.8$ nm. The unidirectional anisotropy constant $K_{eb} = 6.56$ kJ/m^3. Then, the

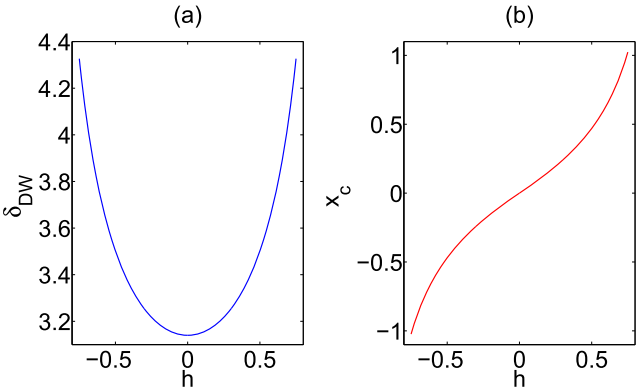

FIG. 3. (a) Domain wall width δ_{DW} and (b) the center position x_c, in the unit of length scale $\sqrt{\frac{A_{ex}}{M_s(H_{ebL}+H_{ebR})}}$, as a function of h.

domain width $\delta_{\rm DW} \simeq \pi\lambda_H = 134$ nm. The energy density is $\gamma_{\rm DW} \simeq 4\sqrt{A_{\rm ex}K_{\rm eb}/2} \simeq 1.12$ mJ/m^2.

Except the exchange energy and the exchange bias energy, there are other types of interactions involved in reality, for example, the dipolar interaction, which is at least one order lower.[18] The shape anisotropy constant $K_{\rm sh} = \mu_0 M_S^2/2 = 0.35$ MJ/m^3 due to demagnetizing energy is much larger than the unidirectional anisotropy $E_{\rm eb} = 6.56$ kJ/m^3 due to exchange bias energy. Although $K_{\rm sh}$ is much larger than $K_{\rm eb}$, in nano-thin, narrow strips, the strong demagnetizing field forces the magnetization vector parallel to the plane of thin, narrow strips so that the exchange bias acts as a slight modulation. This peculiar asymmetric configuration can be obtained experimentally by ion irradiation techniques, by modulating the ion dose for selectively destroying or weakening the exchange coupling between the antiferromagnetic and ferromagnetic layers, and therefore, the exchange bias has asymmetry.[19,20]

IV. UNIAXIAL ANISOTROPY

In this section, we study the effect of in-plane uniaxial anisotropy on the DW structure, its stability, and the depinning field in the one-dimensional wire in the presence of exchange bias.

The in-plane anisotropy should play an important role in determining the domain wall structure and its width. In particular, the domain wall width decreases (increases) if the anisotropy is parallel (perpendicular) to the easy axis.[21–23]

Let $\hat{n}_a = \hat{e}_x \cos\theta_a + \hat{e}_y \sin\theta_a$ be the direction of the easy axis due to uniaxial anisotropy; the magnetization will prefer both θ_a and its reverse direction $\pi - \theta_a$; the anisotropy energy up to the leading order[9] could be represented by

$$E_{\rm ani} = -K_{\rm ani}\int_{-\infty}^{\infty} dx \cos^2(\theta - \theta_a), \tag{22}$$

where $K_{\rm ani} > 0$ is the uniaxial anisotropy constant.[17] Similarly, the spin orientation is obtained by minimizing the total energy, which turns out to be

$$2A_{\rm ex}\frac{d^2\theta}{dx^2} - M_s H_{\rm ebL} \sin\theta - K_{\rm ani} \sin 2(\theta - \theta_a) = 0 \quad \text{if} \quad x < 0, \tag{23}$$

$$2A_{\rm ex}\frac{d^2\theta}{dx^2} + M_s H_{\rm ebR} \sin\theta - K_{\rm ani} \sin 2(\theta - \theta_a) = 0 \quad \text{if} \quad x > 0. \tag{24}$$

In the following, the symmetric bias ($H_{\rm ebL} = H_{\rm ebR} = H_{\rm eb}$) is assumed in order to understand the anisotropic effect. Since no closed form solution of the above-mentioned differential equation is found, we adopt the solution form in Eq. (14) for the case where the anisotropy energy is small compared with the exchange bias energy, i.e., $K_{\rm ani} \ll M_s H_{\rm eb}$. The domain wall length scale $\lambda_{\rm L} = \lambda_{\rm R} = \lambda$ is left as the variational parameter. The total energy becomes

$$\begin{aligned} E &= A_{\rm ex}\int_{-\infty}^{+\infty} {\rm d}x\left(\frac{d\theta}{dx}\right)^2 - \int_{-\infty}^{+\infty} {\rm d}x\vec{H}_{\rm eb}\cdot\vec{M} \\ &\quad + K_{\rm ani}\int_{-\infty}^{\infty} dx \cos^2(\theta - \theta_a) \\ &= 4(2-\sqrt{2})\frac{A_{\rm ex}}{\lambda} + 2(2-\sqrt{2})M_s H_{\rm eb}\lambda \\ &\quad + \frac{4}{3}(4-\sqrt{2})K_{\rm ani}\lambda \cos 2\theta_a. \end{aligned} \tag{25}$$

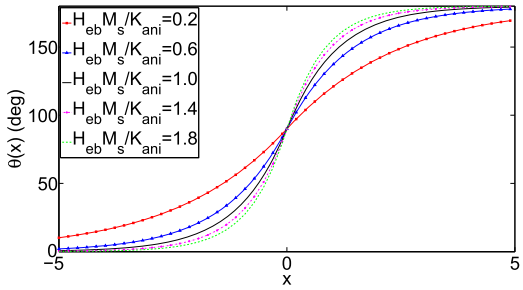

FIG. 4. Spin orientation $\theta(x)$ as a function of x, in the unit of $\sqrt{\frac{A_{\rm ex}}{K_{\rm ani}}}$, for different $\frac{H_{\rm eb}M_s}{K_{\rm ani}}$. $K_{\rm ani} = 10^3$ J/m^3 (along the x-axis).

Minimization with respect to λ gives

$$\lambda = \sqrt{\frac{6A_{\rm ex}}{3M_s H_{\rm eb} + 2(3+\sqrt{2})K_{\rm ani}\cos 2\theta_a}}. \tag{26}$$

To compare with the simulation result,[8] we set the same values of $K_{\rm ani}$ as used in simulation. The spin orientation $\theta(x)$ for different $H_{\rm eb}/K_{\rm ani}$ is shown in Fig. 4. It shows that the larger the anisotropy, the larger the DW width. The domain wall length scale λ (same order of magnitude as the domain wall width) as a function of $H_{\rm eb}$ for different anisotropies is shown in Fig. 5. It can be seen that the difference in DW width for different anisotropies is insignificant if the exchange bias is large enough. It implies that for large exchange bias, the structure of the DW would be slightly modified by the anisotropy effect. Our result is consistent with simulation for which the same plot is shown in Fig. 4(a) in Ref. 8.

If the anisotropy effect takes place along the y-axis, once $K_{\rm ani} \gtrsim M_s H_{\rm eb}$, the domain wall width is sufficiently large such that the boundary condition imposed in Eq. (12) becomes invalid.

If the external magnetic field $\vec{H}_{\rm ext} = H_{\rm ext}\hat{e}_x$ is applied, similar to the case in Sec. III, we could replace $H_{\rm eb}$ by the effective one, i.e., $H_{\rm eb}^{\rm eff} = -H_{\rm eb} + H_{\rm ext}$, in the right side. The solution in Eq. (14) becomes physically unstable when the DW length scale, λ, in Eq. (26) diverges. At this moment, $H_{\rm eb}^{\rm eff} = -H_c + H_{\rm ext}$. It defines the critical

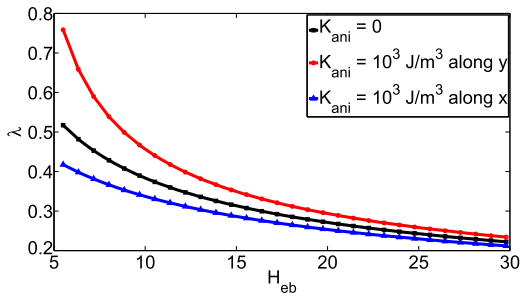

FIG. 5. Domain wall length scale, λ, in the unit of $\sqrt{\frac{A_{\rm ex}}{K_{\rm ani}}}$, as a function of exchange bias field $H_{\rm eb}$ for $K_{\rm ani} = 0$, 10^3 J/m^3 (along the x-axis, $\theta_a = 0$), and 10^3 J/m^3 (along the y-axis, $\theta_a = \pi/2$).

field

$$H_c = H_{eb} + \frac{2(3+\sqrt{2})}{3}\frac{K_{ani}}{M_s}\cos 2\theta_a, \quad (27)$$

which should correspond to the depinning field with the same order of magnitude.

V. CONCLUSION

We analytically solve the spin orientation along the wire in the presence of non-uniform exchange bias,[8] as shown in Eq. (18). Even for symmetry exchange bias field, the solution we get is different from the traditional one, as shown in Eq. (1), which usually appears in the field of micromagnetics.[9]

For asymmetry exchange bias field, the spin orientation θ_0 and the center position of the domain wall x_c as a function of domain wall length scales λ_R and λ_R are also derived analytically. These variables can be easily measured in experiments, and hence, it could be verified in practice. Finally, with a small anisotropic effect, the domain wall stability condition and the depinning field are also obtained.

Although the model is so simplified that only the exchange bias, the exchange energy, and the anisotropy effect are considered, the other contributions from dipolar interactions and the imperfect and edge energy, which are at least one order lower,[18] are ignored; our analytic results are still consistent with previous simulation.[8] The creation and fine tuning of the domain wall by exchange bias and uniaxial anisotropy are shown to be possible. These results should be helpful for the development of new DW-based magnetic devices and architectures.

ACKNOWLEDGMENTS

The authors thank Deng-Shiang Shiu for discussions. The work was supported by the Ministry of Science and Technology of the Republic of China.

DATA AVAILABILITY

Data sharing is not applicable to this article as no new data were created or analyzed in this study.

REFERENCES

[1] S. S. P. Parkin, M. Hayashi, and L. Thomas, Science **320**, 190 (2008).
[2] S. Goolaup, M. Ramu, C. Murapaka, and W. S. Lew, Sci. Rep. **5**, 9603 (2015).
[3] M. Hayashi, L. Thomas, R. Moriya, C. Rettner, and S. S. P. Parkin, Science **320**, 209 (2008).
[4] A. Pushp, T. Phung, C. Rettner, B. P. Hughes, S.-H. Yang, L. Thomas, and S. S. P. Parkin, Nat. Phys. **9**, 505 (2013).
[5] D. M. Burn, M. Chadha, S. K. Walton, and W. R. Branford, Phys. Rev. B **90**, 144414 (2014).
[6] J. Nogués and I. K. Schuller, J. Magn. Magn. Mater. **192**, 203 (1999).
[7] I. Polenciuc, A. J. Vick, D. A. Allwood, T. J. Hayward, G. Vallejo-Fernandez, K. O'Grady, and A. Hirohata, Appl. Phys. Lett. **105**, 162406 (2014).
[8] E. Albisetti and D. Petti, J. Magn. Magn. Mater. **400**, 230 (2016).
[9] J. M. D. Coey, *Magnetism and Magnetic Materials* (Cambridge, 2009), the domain wall structure is discussed in Chapter 7.
[10] J. Shibata, G. Tatara, and H. Kohno, J. Phys. D: Appl. Phys. **44**, 384004 (2011).
[11] C.-Y. You, J. Appl. Phys. **100**, 043911 (2006).
[12] A. Aharoni, J. Appl. Phys. **83**, 3432 (1998).
[13] M. D. DeJong and K. L. Livesey, Phys. Rev. B **92**, 214420 (2015).
[14] A. Hoffmann, M. Grimsditch, J. E. Pearson, J. Nogués, W. A. A. Macedo, and I. K. Schuller, Phys. Rev. B **67**(R), 220406 (2003).
[15] Y. Du, G. Pan, R. Moate, H. Ohldag, A. Kovacs, and A. Kohn, Appl. Phys. Lett. **96**, 222503 (2010).
[16] Strictly speaking, $\pi(\lambda_L + \lambda_R)/2$ is not exactly the domain wall width because the magnetization direction only asymptotically approaches 0 or π. However, we could still define the width as its corresponding length scale $(\lambda_L + \lambda_R)/2$ multiplied by a constant π. This proportionality constant is adopted to be consistent with the usual definition. See Eq. (7.16) in Ref. 9.
[17] K. O'Grady, L. E. Fernandez-Outon, and G. Vallejo-Fernandez, J. Magn. Magn. Mater. **322**, 883 (2010).
[18] K. J. Kim and S. B. Choe, J. Magn. Magn. Mater. **321**, 2197 (2009).
[19] A. Mougin, S. Poppe, J. Fassbender, B. Hillebrands, G. Faini, U. Ebels, M. Jung, D. Engel, A. Ehresmann, and H. Schmoranzer, J. Appl. Phys. **89**, 6606 (2001).
[20] E. Albisetti, D. Petti, M. Pancaldi, M. Madami, S. Tacchi, J. Curtis, W. P. King, A. Papp, G. Csaba, W. Porod, P. Vavassori, E. Riedo, and R. Bertacco, Nat. Nanotechnol. **11**, 545 (2016).
[21] D. G. Porter and M. J. Donahue, J. Appl. Phys. **95**, 6729 (2004).
[22] M. T. Bryan, S. Bance, J. Dean, T. Schrefl, and D. A. Allwood, J. Phys.: Condens. Matter **24**, 024205 (2012).
[23] R. Hertel and A. Kákay, J. Magn. Magn. Mater. **379**, 45 (2015).